

RESEARCH ARTICLE

10.1002/2017GC007215

Pervasive Eclogitization Due to Brittle Deformation and Rehydration of Subducted Basement: Effects on Continental Recycling?

Key Points:

- Extensive rehydration of continental basement during subduction was quantitatively documented in the Sesia Zone (Western Alps)
- Following brittle deformation, repeated pulses of high-pressure fluid infiltrated and converted felsic granulites to eclogitic micaschists
- Modeling indicates density separation during subduction, suggesting that composition controls which units escape upward and which of them descend to a subduction graveyard

Supporting Information:

- Supporting Information S1

Correspondence to:

M. Engi,
engi@geo.unibe.ch

Citation:

Engi, M., Giuntoli, F., Lanari, P., Burn, M., Kunz, B., & Bouvier, A.-S. (2018). Pervasive eclogitization due to brittle deformation and rehydration of subducted basement: Effects on continental recycling? *Geochemistry, Geophysics, Geosystems*, 19, 865–881. <https://doi.org/10.1002/2017GC007215>

Received 5 SEP 2017

Accepted 29 JAN 2018

Accepted article online 1 MAR 2018

Published online 23 MAR 2018

Martin Engi¹ , Francesco Giuntoli^{1,2} , Pierre Lanari¹ , Marco Burn¹, Barbara Kunz¹ , and Anne-Sophie Bouvier³

¹Institute of Geological Sciences, University of Bern, Bern, Switzerland, ²School of Geography, Earth and Environmental Sciences, Plymouth University, Plymouth, UK, ³SwissSIMS, Université de Lausanne, Géopolis, Lausanne, Switzerland

Abstract The buoyancy of continental crust opposes its subduction to mantle depths, except where mineral reactions substantially increase rock density. Sluggish kinetics limit such densification, especially in dry rocks, unless deformation and hydrous fluids intervene. Here we document how hydrous fluids in the subduction channel invaded lower crustal granulites at 50–60 km depth through a dense network of probably seismically induced fractures. We combine analyses of textures and mineral composition with thermodynamic modeling to reconstruct repeated stages of interaction, with pulses of high-pressure (HP) fluid at 650–670°C, rehydrating the initially dry rocks to micaschists. SIMS oxygen isotopic data of quartz indicate fluids of crustal composition. HP growth rims in allanite and zircon show uniform U-Th-Pb ages of ~65 Ma and indicate that hydration occurred during subduction, at eclogite facies conditions. Based on this case study in the Sesia Zone (Western Italian Alps), we conclude that continental crust, and in particular deep basement fragments, during subduction can behave as substantial fluid sinks, not sources. Density modeling indicates a bifurcation in continental recycling: Chiefly mafic crust, once it is eclogitized to >60%, are prone to end up in a subduction graveyard, such as is tomographically evident beneath the Alps at ~550 km depth. By contrast, dominantly felsic HP fragments and mafic granulites remain positively buoyant and tend to be incorporated into an orogen and be exhumed with it. Felsic and intermediate lithotypes remain positively buoyant even where deformation and fluid percolation allowed them to equilibrate at HP.

Plain Language Summary Processes inside subduction zones are fundamental for continental accretion and the recycling of the Earth’s crust into the mantle, but many aspects remain poorly understood. As tectonic plates converge, continental rocks resist subduction into the denser mantle, except where they are transformed to high-pressure mineral assemblages. This densification process is known to be particularly sluggish for dry rocks. We document that tectonic bodies of dry continental crust now in the Western Alps were extensively (re)hydrated during subduction. The effects of brittle deformation, providing access to hydrous fluids at >60 km depth, is investigated by detailed petrology, U-Th-Pb geochronology, oxygen isotopes, and modeling of phase equilibria. These results - combined with density modeling and then scaled up - suggest that, unless hydration occurs, continental crust may undergo density separation beneath the overlying plate. A dense layer at ~550 km depth, visible by tomography beneath the Western Alps, is interpreted as a subduction graveyard that separated from the hydrated rocks documented in this study.

1. Introduction

Fluids are major players in subduction processes, but their game remains poorly understood, especially in continental slabs. Thermal breakdown of hydrous minerals will liberate fluids, and these can trigger processes as diverse as seismic failure (Abers et al., 2013; Barcheck et al., 2012), mantle infiltration (Soret et al., 2016), or hydrous melting (Labrousse et al., 2015). But continental slabs comprise mostly pretty infertile lithotypes, with sparse hydrates, and little is known about how fluids in the subduction channel interact, especially with very dry rocks (Angiboust et al., 2017) before these reach their solidus.

Studies of HP rocks in several orogens have concluded that hydrous fluids profoundly change how rocks of the continental lower crust are deformed and to what extent they are transformed to eclogite by mineral reactions. Such densification is known to be sluggish in dry rocks (Wain et al., 2001), but kinetic barriers

(Bjørnerud et al., 2002; Hetényi et al., 2007) can be reduced by the combined effects of deformation and fluid flow (Austrheim, 1987; John & Schenk, 2003; Lund & Austrheim, 2003). It is not clear to what extent tectonic fragmentation happens near a subduction interface, how interaction with fluids is likely to occur, and how coupling with deformation changes the tectonic flow. Results from numerical models (Gerya et al., 2002; Warren et al., 2008) indicate that tectonic mixing may occur in a subduction channel, but the styles and spatial-temporal scales proposed require testing.

It is clear that the Earth's continental crust has evolved by tectonic recycling of lithospheric materials and that subduction plays a major role in this process (Hacker et al., 2011). Seismic tomography beneath various fossil convergent margins indicates lithospheric fragments residing at mantle depths (Lippitsch et al., 2003; Replumaz et al., 2010), but such geophysical probing provides little control on composition. Conversely, the analysis of high-pressure rocks in orogens yields detailed insight, but crustal fragments buried in the mantle are missing there. Continental rocks, owing to their compositional diversity, experience substantial differences in buoyancy and rheology relative to other lithotypes, notably mantle rocks. The combined effects of such differences on recycling processes remain poorly understood, but they are likely significant at convergent plate margins.

This is particularly true where a previously extended (passive) plate margin gets involved in continental subduction, as is the case in the Alps (Beltrando et al., 2014; Mohn et al., 2014). Extensional faults can expose middle to lower crustal fragments composed of dry rock types, with very little or no sedimentary cover. Once convergence starts, such faults are readily reactivated, entraining flat-lying fragments into subduction. Within the subduction channel, dry rocks show substantially different flow and rupture characteristics than upper crustal materials, notably sediments. The latter produce fluids by metamorphic dehydration during subduction and can promote densification reactions.

The present study aims to clarify the combined effects of deformation and fluids in the Sesia Zone (Italian Western Alps) within a well-constrained temporal setting. This continental terrain stands out for its extensive eclogitization, compared to similar terrains (e.g., Western Norway), but the causes of this pervasive HP imprint await an explanation. We document repeated fluid-access related to a network of brittle fractures, and we quantify and date the detailed small-scale processes by which previously dry rocks were (re)hydrated and pervasively transformed at eclogite facies conditions. We then use density modeling to explore the effectiveness of densification for realistic continental lithotypes. The results indicate that, at lithosphere scale, buoyancy differences persist for upper and lower crustal fragments, contributing to flow separation into eclogites emerging (in orogens) versus incorporation into a slab graveyard in the mantle.

2. Materials and Methods

Over 100 samples of eclogitic micaschists were initially investigated by petrography to select those best suited for detailed analysis by petrochronological and geochemical methods.

2.1. Geodynamic and Geological Framework of Samples

The Sesia Zone is an internal segment of the Western Alps that formed during convergence of the European and the African plate in the upper Cretaceous. Preceding subduction and Alpine orogeny, extension had produced a continent-ocean transition zone and the Tethys Ocean. As explained in more detail in supporting information (supporting information Figure S1), the transition zone probably involved listric faults separating basement fragments that had been rifted off the NW-margin of the Adriatic microplate. In the Southern Alps, notably the Ivrea Zone, some of the intact Adriatic basement is preserved, for it was part of the upper plate and thus completely escaped subduction.

The Sesia Zone in the Western Alps, famed for its spectacular eclogites, has long been viewed as related to the Ivrea Zone (Southern Alps), which in turn is best known for Permian granulites and mafic intrusives. The Sesia Zone is part of a classic Alpine thrust sheet, termed as the Sesia-Dent Blanche nappe, composed of high-pressure (HP) blueschist to eclogite facies rocks, most of them continental and polycyclic (Dal Piaz, 1999; Manzotti et al., 2014). HP metamorphism in the Sesia Zone reflects SE-directed subduction, with km-size fragments reaching depths of ~55 to 60 km at different stages, between ~85 and 65 Ma ago (Regis et al., 2014; Rubatto et al., 2011). Remarkably, these continental basement units became a coherent nappe 65–60 Ma ago and were amalgamated, following partial exhumation, with the upper plate while subduction

jumped westward. Only then were parts of the Tethys (Ligurian ocean) subducted, reaching HP conditions 58–40 Ma ago (Weber et al., 2015). Note that this age sequence is opposite to the usual pattern—oceanic subduction first, continental units next. A likely cause is that flat-lying extensional faults represent weak discontinuities that were reactivated first during convergence (Mohn et al., 2014).

In detail, central parts of the Sesia Zone comprises two main complexes, i.e., the Internal and External Complexes (IC and EC hereafter; Giuntoli & Engi, 2016), which are separated by a greenschist facies shear zone. The IC consists of several eclogitic units, each 0.5–3 km thick, separated by presumed monometamorphic (Mesozoic) metasediments (Giuntoli & Engi, 2016; Regis et al., 2014). This highly deformed complex is characterized by interlayered micaschist, eclogite, orthogneiss, and paragneiss, with a minor portion of pre-Alpine marbles and (probably) Mesozoic metasedimentary trails (e.g., Compagnoni, 1977). The IC experienced eclogite facies conditions during Alpine metamorphism, with maximum recorded pressure of 2 GPa and temperature of 650–670°C, between 85 and 55 Ma (Compagnoni, 1977; Konrad-Schmolke et al., 2011a; Regis et al., 2014; Rubatto et al., 2011). The IC preserves rare relics of pre-Alpine (Permian) granulite (0.6–0.9 GPa, ~850°C) and retrograde amphibolite conditions (0.5–0.3 GPa, 570–670°C; e.g., Lardeaux & Spalla, 1991; Zucali et al., 2002). The EC comprises three epidote blueschist facies sheets of orthogneiss, with only minor paragneiss and metasediments, which are separated by lenses and trails of partially overprinted pre-Alpine high-temperature rocks.

2.2. Methods Used

Except where indicated below, all instruments used are at the Institute of Geological Sciences, University of Bern (Switzerland). Details of analytical procedures are given in supporting information Methods.

For mineral separation, rock samples were disaggregated in a Selfrag apparatus, which produced a high yield of intact mineral grains by high-voltage pulsing to a grain size of ~250 μm. Sieved fractions (usually ϕ 60–500 μm) were then separated using classical magnetic and heavy liquid techniques to obtain allanite and zircon grains for isotopic analysis.

Mineral analyses and X-ray maps were obtained by electron probe microanalysis (EPMA using a Jeol JXA-8200), Th-U-Pb isotopic analysis of allanite and zircon by LA-ICP-MS (using a Geolas Pro 193 nm ArF excimer laser coupled to an Elan DRC-e quadrupole ICP-MS).

Oxygen isotopic data of quartz were obtained by SIMS using the Cameca IMS 1280-HR instrument at the Swiss-SIMS national facility, Université de Lausanne, Switzerland.

Owing to the complexity in local textures, it was essential to select appropriate locations for microanalysis by EPMA, LA-ICP-MS, and SIMS. Compositional maps generated by XMapTools (Lanari et al., 2014) were indispensable to retain precise contextual links, without which spot analyses and age data would not have been interpretable.

Whole-rock compositional data were obtained by XRF at the University of Lausanne, using a PANalytical PW2400 spectrometer. Loss-on-ignition (LOI) was determined on rock powders by weight difference after 90 min of ignition at 1,050°C.

3. Formation of Eclogitic Micaschists Involved Pulses of HP Fluid and Mineral Cannibalism

3.1. Bulk Rock Geochemistry

To trace the origin of these micaschists, we determined the geochemical characteristics of the sample material. Major element concentrations were analyzed of 18 micaschists selected for this study; 16 of these were taken in the IC of the Sesia Zone; two similar samples are from the more external Emilius klippe. Our data are analyzed jointly with published analyses for micaschists from the IC. Irrespective of the source, all data for eclogite-facies samples indicate clastic sedimentary protoliths, with high K_2O/CaO ratios (median: 2.2) and low calcium contents (median: 1.5 wt % CaO), hence rocks that contained very minor or no carbonate. The Chemical Index of Alteration (Nesbitt & Young, 1982) (defined as $100 \times Al_2O_3 / (Al_2O_3 + K_2O + Na_2O + CaO)$, molar units) varies from 52 to 81 (median: 65), implying a clastic series ranging from impure quartzite to mature shale. This is consistent with what the data indicate in an AFM-plot (Figure 1), i.e., a range from immature to mature clastic sediments, with pelites dominating. However, the scatter in

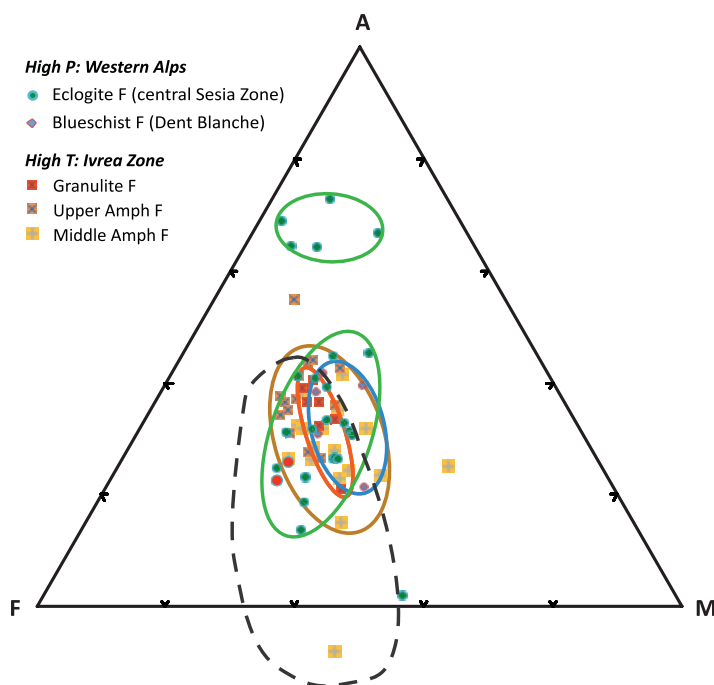


Figure 1. Chemical characteristics of clastic metasediments. AFM projection of geochemical data for high-pressure micaschists from the Western Alps. Data from this study, from Konrad-Schmolke et al. (2011b) and Regis (2012) for Sesia Zone (eclogite grade, green ellipses), from Diehl et al. (1952) and Höpfer (1997) for Dent Blanche (blueschist facies, blue ellipse). Red symbols mark Sesia samples (FG1249, FG1315) detailed in this paper. Dashed outline delimits typical shale compositions and indicates that the spread of all data reflects similar clastic sedimentary protoliths. Also shown are data from Redler (2011) for upper amphibolite (brown ellipse) to granulite (red ellipse) grade rocks in the Ivrea Zone; these correspond to high-temperature precursors of the micaschists. F: Facies.

data sets from metasediments may not be directly interpretable as a range in source rock compositions, since part of the variability may be due to metamorphic mass transfer.

To test potential genetic relations of the micaschists in the Sesia Zone with those in cognate tectonic units (at different metamorphic grade), we compare their chemical composition. In the Dent Blanche unit, i.e., a lower-grade part of the same Alpine thrust sheet as the Sesia Zone (Manzotti et al., 2014), high-pressure samples (at blueschist facies) show less scatter in Figure 1 than those in the Sesia Zone, but they appear otherwise comparable. Likewise, data from the Ivrea Zone (part of the Adriatic margin that escaped an Alpine high-pressure overprint) are similar in the AFM diagram. We note a minor but distinct group of more aluminous compositions in the Sesia data, not evident in other data sets, and with an apparent gap or offset from more typical pelitic compositions. Apart from these very Al-rich samples and a small number of isolated compositional outliers, the fields outlined in Figure 1 for each unit show very similar geochemical features. The median compositions of metasediments analyzed from each unit are almost identical in AFM and certainly compatible with the notion of initially related clastic source rocks.

Major differences emerge, however, in the volatile contents of these same samples, as expected from their variable metamorphic imprint. Volatile contents (in supporting information Tables S1 and S2) vary from 1.4 to 3.1 wt % LOI; loss-on-ignition mostly corresponds to the hydroxide-contents of several metamorphic silicates (chiefly phengite, epidote, glaucophane), though a minor fraction may reflect hydrous fluid inclusions. Compared to the sedimentary protoliths, in which clay minerals were the main water carriers, metamorphic dehydration reactions clearly reduced the volatile contents by several weight %. All of the data sets compared in Figure 2 are from metasediments in tectonic units that experienced similar thermal histories up to the late

Paleozoic. The trend evident from the median LOI values in the Ivrea Zone (left) is due to metamorphic dehydration, from ~1.6 to ~0.4 wt %. In tectonic units of the Western Alps (right part of diagram), LOI data show an increase with subduction depth and temperature attained. The *HP* overprint resulted in volatile contents that reach a median LOI ~1.5% in blueschist facies terrains, and about 2.0% at eclogite facies. For all of the geochemical data as well as for the PT estimates, data and sources are listed in supporting information Tables S1 and S2.

3.2. Petrological and Petrochronological Data, Oxygen Isotopes

3.2.1. Detailed Petrography of Micaschists

Individual samples of Sesia micaschists show remarkable textural features that provide insight into mechanisms and effects of fluid-rock interaction at high pressure. The most spectacular observations concern garnet, but zircon and quartz add important evidence (see below).

Petrographically, the micaschists are well foliated and often show banding at mm-scale to cm-scale. Fabrics indicate polyphase and generally strong deformation (see supporting information Figure S2). Mineral assemblages in the metasediments vary little, but phases occur in highly variable relative proportions. Overall, quartz and white mica (phengite ± paragonite) make up 60–90%, with garnet, sodic amphibole (glaucophane), epidote, and rutile plus accessory allanite and zircon. Associated eclogite bands or lenses contain varying amounts of omphacite, glaucophane, garnet, phengite, epidote, quartz, and rutile (Giuntoli & Engi, 2016).

In thin section, mineral fabrics appear well equilibrated, with a foliation described by alternating submillimetric bands of phengite + paragonite and quartz showing crystals with a shape preferred orientation aligned in the foliation. Prisms of allanite and rutile are aligned in the foliation, whereas the more isometric

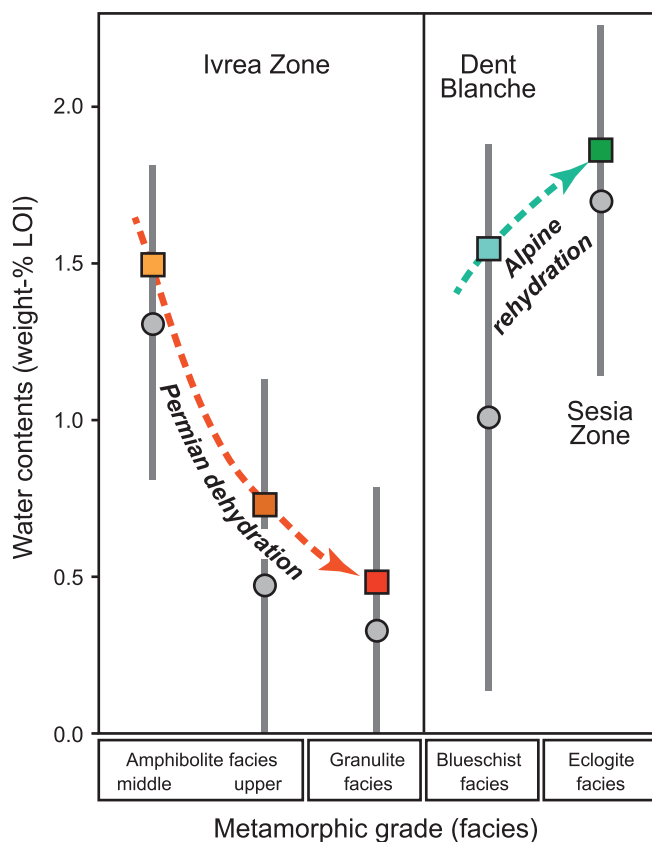


Figure 2. Volatile contents of metapelites. Loss-on-ignition (LOI) data of 76 samples from seven metamorphic units shown as a function of metamorphic grade (pressure along abscissa). Squares mark the median LOI, circles the mean ($\pm 1SD$ error bars), temperatures from thermobarometry. Arrows indicate two distinct trends; (left) LOI decreased by Permian heating and burial; (right) water contents increased with depth attained during Alpine subduction. Raw data and sources in supporting information Table S1. Note the asymmetry in all LOI data sets: the median is above the mean, indicating that low LOI values are rare exceptions in the data set.

garnet grains are wrapped by it. Minor chlorite, albite, and actinolite locally occur as retrograde greenschist facies minerals, as do epidote rimming allanite and titanite rimming rutile.

At grain-scale, mutual inclusions, overgrowths, and chemical zoning, even in the fresh HP assemblages, show complexities, revealing evidence of several successive stages of deformation and local mineral growth or replacement. Particularly striking overgrowth textures are seen in garnet, and details about these are analyzed below, as they give important clues about the samples' history. As mineral assemblages are used to quantify the pressure-temperature (P-T) conditions at which they formed, it is essential to identify which phases found in a microscopic domain of the sample reflect which stage of its evolution and what the compositions of coexisting phases are. Data and observations detailed in this paper are restricted to few samples, but we stress that these are typical, and we have observed similar features in many micaschists from the central Sesia Zone.

3.2.2. Garnet

In many thin sections, garnet was observed as two very different microtextural types. Detailed data are here presented for sample FG1315 (Figures 3–7), as it is typical of the suite of micaschists analyzed: Gar-1 crystals (\varnothing 4–8 mm) preserve a densely fractured porphyroclastic core and up to three overgrowth zones; Gar-2 are smaller garnet (\varnothing 50–300 μm), typically with an atoll structure. Individual samples show local variations, but the sample discussed here is typical: FG1315 contains cores of Gar-1, which are optically bright and contain inclusions of ilmenite (in part transformed to rutile). The first two overgrowths (rim-1 + rim-2) are cloudy due to finely dispersed rutile inclusions; outer overgrowths (rim-3) are bright and contain few inclusions of coarse rutile. Quartz inclusions are abundant inside rim-1 and between rim-1 and rim-3, but are absent within rim-2. Atoll-type garnet (Gar-2) is optically bright; its core is now filled by quartz and/or minor phengite. In both types of garnet, minor chlorite occurs, but only along brittle fractures; hence, it is considered a late feature.

Standardized X-ray maps for garnet end members (Lanari et al., 2014) reveal morphologically and chemically complex zoning (Figure 3).

Compositional boundaries are sharp, with no diffusional broadening visible at electron microprobe scale (beam \varnothing : $\sim 1 \mu\text{m}$). Changes in chemical composition across these boundaries are abrupt and systematic, indicating discrete steps of growth (and/or dissolution), with minimal variability inside each zone. The spatial distribution of individual growth zones and their irregular shapes are incompatible with simple overgrowth, i.e., mere peripheral addition of garnet. Instead, partial replacement is indicated by tongues of identical composition, which are present both inside and outside the grain perimeter.

A map of the calcium concentration (mole fraction of the grossular endmember X_{Grs} in Figure 3a) shows a porphyroclastic core ($X_{\text{Grs}} \approx 0.03$) with a lobate structure and numerous fractures that are sealed by more calcic garnet ($X_{\text{Grs}} \approx 0.09$). A first rim around the relic core is higher yet in calcium ($X_{\text{Grs}} \approx 0.18$); this rim is thinner in the direction of the main foliation and produced peninsular growths within the core, clear evidence of a replacement process. A second stage rim, with $X_{\text{Grs}} \approx 0.12$, grew on both sides (i.e., internally and externally) of rim-1, with morphological evidence of resorption at the expense of rim-1 and of the core: rim-1 shows fine fractures that are sealed by rim-2, and rim-2 also surrounds the rim-1 peninsula in the core. The outermost rim (rim-3) is lower in calcium ($X_{\text{Grs}} \approx 0.055$) and clearly resorbed or replaced the previous rims, producing peninsular growths inside rim-1. Stage-3 seems not to have affected the core. Rim-3 is thicker perpendicular to the main foliation, along which fluids are likely to have migrated.

In different micaschist samples studied, analogous features were found, though the shapes and compositions of individual evolutionary zones vary somewhat. One important variable is grain size, as the example

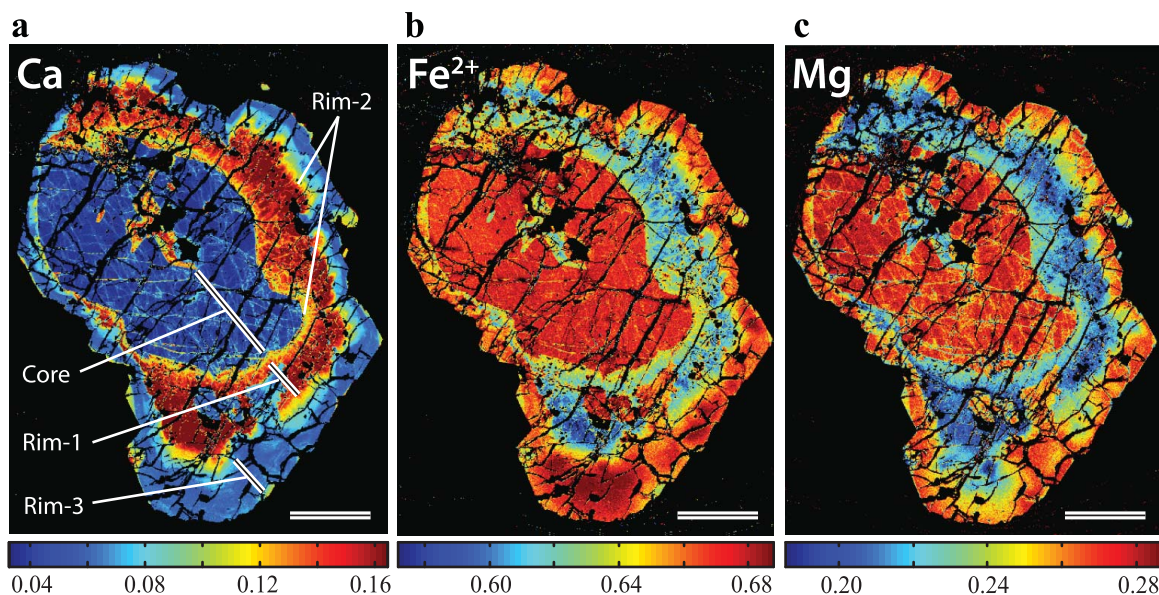


Figure 3. Compositional maps of a garnet grain: core with several rims. Compositional maps of garnet endmembers, sample FG1315: (a) X_{Grs} (Ca), (b) X_{Alm} (Fe^{2+}), and (c) X_{Prp} (Mg); mole fraction scales at the base. Zoning shows a corroded core and a sequence of rims. Note the dense network of healed hairline fractures (1–3 μm wide) in the core and rim-1. Complex intergrowth textures indicate repeated cannibalism: Later garnet overgrew and partly replaced earlier garnet. Quartz inclusions appear black, as do coarse cracks of secondary chlorite (seams $\sim 15 \mu\text{m}$). Scale bar: 400 μm .

of atoll garnet shows. These occur in FG1315, side by side with the porphyroclastic type just described, but in separate layers of lesser grain size. Zoning patterns in the two types (Figure 7) are partly analogous, with notable deviations. In atoll garnet, resorption of the core is locally visible already at stage-1. Remarkable negative crystal forms remain at the inner growth surface of stage-1, with overgrowths of stage-2 being limited to the then outer surface. Complete resorption of the core, i.e., formation of the atoll structure, certainly postdates stage-1 and probably also stage-2. Quartz or coarse phengite, completely unstrained, now occupy the space inside the garnet rims, i.e., small garnet cores have been completely replaced.

The larger cores, preserved inside the porphyroclastic types of garnet, show a much more modest, but significant replacement feature. The dense network of hairline fractures in garnet was healed by thin seams of garnet. As they are only 1–3 μm wide, their composition is difficult to analyze precisely, but EPMA data indicate that the fracture fillings are comparable to rim-1 or rim-2.

Before developing a model of this zonal sequence in garnet, we present data for zircon, allanite, and quartz.

3.2.3. Zircon

Zircon, much like garnet, commonly preserves texturally identifiable details, even under extreme geological conditions, and textures often reflect polyphase growth. Because of its robust qualities, zircon is a workhorse in geochronology, suitable for documenting the age of successive metamorphic stages. In order to date complex zircon in high-pressure rocks, overgrowth and dissolution features are frequently observed, hence detailed imaging and in situ isotopic analysis is indispensable (Rubatto & Hermann, 2007). We separated single grains of zircon from our samples and studied them by SEM, using cathodoluminescence (CL) imaging to document their internal textures. Results for sample FG1315 in Figure 4 reveal complex internal features, with evidence of dissolution and polyphase metamorphic overgrowth. A variety of cores are found, some are rounded clasts indicating sedimentary protoliths, some show oscillatory zoning (Figure 4d) in growth domains, typical of a magmatic origin. LA-ICP-MS spot ages of cores range from ca. 700 to 350 Ma. Cores typically are coated by one or two CL-grey rims of uneven thickness, followed by a dominant CL-bright growth zone. The latter corroded and partly replaced the inner grey rim(s), locally also inundating the core (Figure 4e). Both the bright and the inner grey rims are Permian (in a, f) growth stages. Comparable CL-characteristics and trace element contents were reported from the Ivrea Zone (Vavra et al., 1996); that study proposed a hydrothermal origin for the CL-bright rims and attributed the corrosion to surface alteration processes. In FG1315, the CL-bright growths are variably preserved, their outer surface is typically rounded or shows highly variable amounts of resorption: From an equant morphology (in d) with only

minor pits, to ~50% missing (in a–c), to almost completely resorbed (in f). The rims deposited on the CL-bright Permian growth zones, and in part replacing them, reflect several stages of Alpine metamorphism (spot ages in a, b, d, and f). These peripheral growths again show mutual (internal) corrosion features, indicating repeated surface controlled interaction with a chemically reactive fluid (Geisler et al., 2007).

Based on sample FG1315, the zircon U-Pb ages shown in Figure 4, combined with PT data in supporting information Table S4 constrain the Permian HT metamorphism at ~290 Ma. The ages shown for the Alpine overgrowth rims cannot be precisely linked to the metamorphic evolution. They cover a range from 62 to 65 Ma, perfectly in line with zircon ages from other Sesia samples (Giuntoli et al., 2018; Rubatto et al., 1997).

3.2.4. Allanite

Allanite is found in many eclogitic micaschists such as FG1315, and in various samples spot dating by Th-Pb and U-Pb methods combined with microtextural analysis has allowed metamorphic stages to be distinguished (Engi, 2017; Janots et al., 2009; Regis et al., 2014; Rubatto et al., 2011). Of central importance are tight links of in situ age data to the metamorphic grade and structural evolution of the samples, and the presence of characteristic inclusions (e.g., of phengite, omphacite, garnet) in allanite can provide such links. While allanite geochronology involves various problems, allanite age data have greatly aided in clarifying the timing of metamorphic processes (Gregory et al., 2012; Hermann & Rubatto, 2003; Janots et al., 2009), especially when combined with data from zircon or monazite.

In sample FG1315, metamorphic allanite includes garnet (Figure 5a) that corresponds in composition to rim-2 or rim-3 (Figure 3) hence allanite grew at or after rim-3 of garnet (quantified below). Phengite inclusions have the same composition as the white mica in the matrix that defines the main Alpine foliation, and allanite prisms and their phengite inclusions grew in alignment with that main penetrative foliation. Allanite grains are of suitable size and homogeneity for dating by LA-ICP-MS, yielding an average $^{238}\text{U}/^{206}\text{Pb}$ Tera-Wasserburg age of 65.0 ± 3.6 Ma (Figure 5; $^{208}\text{Pb}/^{232}\text{Th}$ isochron age 65.9 ± 4.5 Ma); both are within error of the spot ages obtained on zircon (Figure 4) (data in supporting information Table S6).

3.2.5. Quartz

The oxygen isotopic composition of *quartz* can be used to trace interactions with fluid (Li et al., 2001). Quartz in our samples is similar to garnet in that it occurs in different textural settings that reflect several stages in the rock evolution. Depending on the samples, 3–4 different textural domains could be identified by petrography.

We extracted these quartz domains from two thin sections and measured their oxygen isotope compositions by SIMS. Prior to isotopic analysis, we first selected quartz grains from each sample, using petrographic criteria to group them according to relative age: (a) Roundish grains and aggregates of quartz, completely included in earliest garnet (porphyroclasts), were identified as potentially representing relics of the pre-Alpine HT quartz; subsequently younger generations were (b) polygonal bands and lenses made of large (locally undulose) quartz grains sandwiched between phengite-rich aggregates; such quartz is thought to represent a generation that recrystallized (at least partly) during an early phase of rehydration; (c) small grains of well recrystallized quartz in the periphery of late-stage garnet overgrowths and in their pressure shadows, as well as around small, late-stage garnet are interpreted to have partially recrystallized in the presence of a fluid; (d) quartz inside the cores of atoll garnet is likely to reflect late reactive interaction with fluid. Quartz grains of each group were then drilled out and mounted for isotopic analysis (data listed in supporting information Table S5).

The $\delta^{18}\text{O}$ values for quartz in Figure 6a indicate two important features. First, grain-scale heterogeneity in $\delta^{18}\text{O}$ is preserved in most of the quartz domains. In both samples, analyses at small scale—even within some of the larger single quartz grains—shows variations (in Figure 6a) that exceed the analytical uncertainty of the SIMS data. Some diffusional homogenization could be expected at temperatures near 600°C, but the observed variability implies that oxygen diffusion was too slow to allow homogenization at grain scale. Second, in both samples, the median $\delta^{18}\text{O}$ values show a minor change over time (from left to right in Figure 6b), i.e., an evolution from the texturally oldest types of quartz to the latest ones. Quartz extracted from inside the oldest garnet relics in sample FG1315 are almost constant, indicating that they were essentially screened from fluids. In FG1249, the protection evidently was less perfect, as a few grains already show lower $\delta^{18}\text{O}$. The subsequently younger generations show more substantial changes in $\delta^{18}\text{O}$ in both samples, but in all data sets some of the spots essentially preserve isotopic values as heavy as group (a). In

old quartz bands (group b), the deviation measured for most grains is still small. Matrix quartz grains (group c) show much more deviation on average, and some spots deviate substantially from values in group (a). In FG1315, the grains most affected in each group show spots with sequentially more decrease in $\delta^{18}\text{O}$. With the exception of four spots (right-most symbols in b), all of the data show a stepwise trend approaching a $\delta^{18}\text{O}$ value of $\sim 14.1\text{‰}$. The four exceptional spots were all measured in a single quartz grain from the core part of an atoll garnet. While variability from one fluid pulse to the next cannot be excluded, the overall trends for both samples are consistent with an external fluid of uniform oxygen isotopic composition ($\delta^{18}\text{O} \sim 14.1\text{‰}$). Only in sample FG1315, the last four spots show lower $\delta^{18}\text{O}$, so late quartz inside atoll garnet evidently formed from a lighter fluid ($\delta^{18}\text{O} < 13.4\text{‰}$).

Data for the second sample (FG1249 containing no atoll garnet) show a less pronounced but similar trend within and among groups. However, in this case, the final $\delta^{18}\text{O}$ value of $\sim 14.1\text{‰}$ is approached from initially lighter oxygen compositions. Note that $\delta^{18}\text{O}$ values of the earliest quartz, which may have equilibrated with garnet during the Permian) is $\sim 15.2\text{‰}$ in sample FG1315, but $\sim 13.5\text{‰}$ in FG1249. If interaction with a fluid of constant oxygen isotopic composition ($\sim 14.2\text{‰}$) was indeed responsible for the observed trends, FG1315 experienced a decrease in $\delta^{18}\text{O}$ by $\sim 1.1\text{‰}$, whereas FG1249 saw an increase by $\sim 0.6\text{‰}$. The greater discrepancy in $\delta^{18}\text{O}$ values between earliest and latest quartz in FG1315 may explain the steeper trend for matrix quartz compared to FG1249. Experimentally determined fractionation coefficients of oxygen isotopes between quartz and water (Clayton et al., 1972; Matthews & Beckinsale, 1979) are very close to unity at temperatures above 500°C ; hence, the oxygen isotopic composition of an infiltrating aqueous fluid is essentially the same as that of quartz when the two phases are in isotopic equilibrium.

These temporal trends document incomplete isotopic equilibration between high-grade metasediments and several pulses of hydrous fluid of crustal composition. At the time when most interaction took place, $\delta^{18}\text{O}$ of these fluids may have been uniform.

4. Modeling: Extent of Garnet Cannibalism and P-T History

The modeling results for each stage analyzed in FG1315 are shown in Figure 7, and similar data were presented by Lanari et al. (2017), who also detail the modeling approach used. Based on the whole-rock composition determined by XRF analysis, the garnet composition observed in the relic cores is predicted to be thermodynamically stable at PT conditions of 0.7–0.8 GPa and $720\text{--}780^\circ\text{C}$ (data and model results in supporting information Tables S3 and S4). These conditions are completely at odds with those found for the Alpine HP metamorphism in the Sesia Zone: Alpine pressures are twice as high, temperatures are 150--

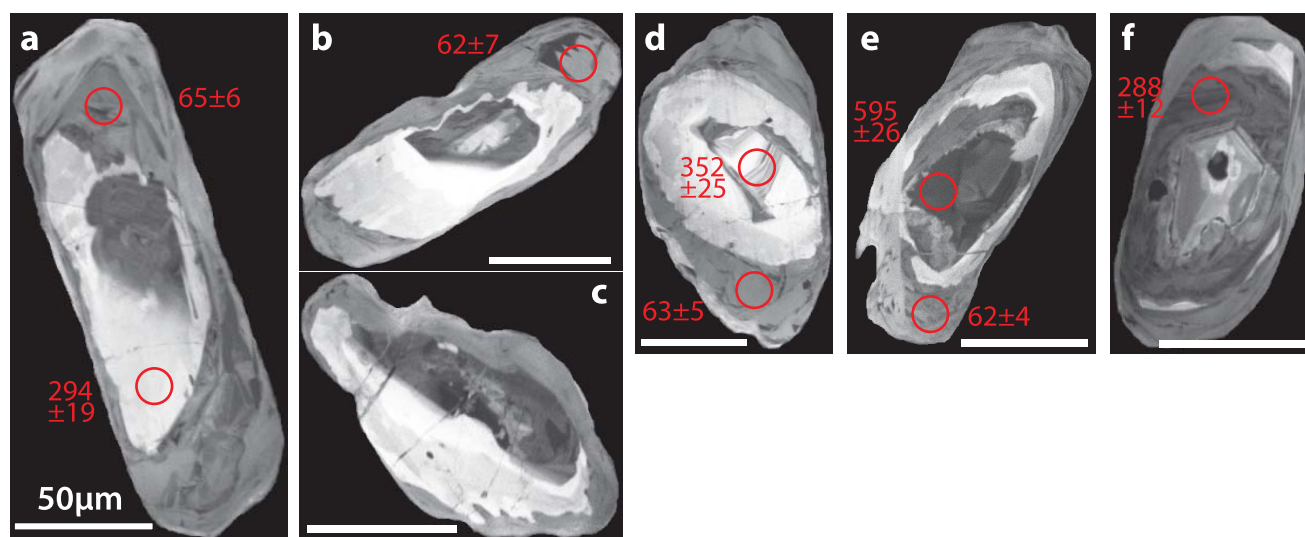


Figure 4. Internal morphology and spot ages of zircon grains. Cathodoluminescence images, sample FG1315. Some cores contain detrital relics (LA-spot age in d, e). Widest Permian growth zones (with ages shown in a, f) are embayed and partly missing (c, e, f). Peripheral grey rims are Alpine overgrowth stages (spot ages in a, b, d, e). Spot ages shown are uncorrected $^{206}\text{Pb}/^{238}\text{U}$ (Ma, $\pm 2\text{s.e.}$). Red circles mark laser spots.

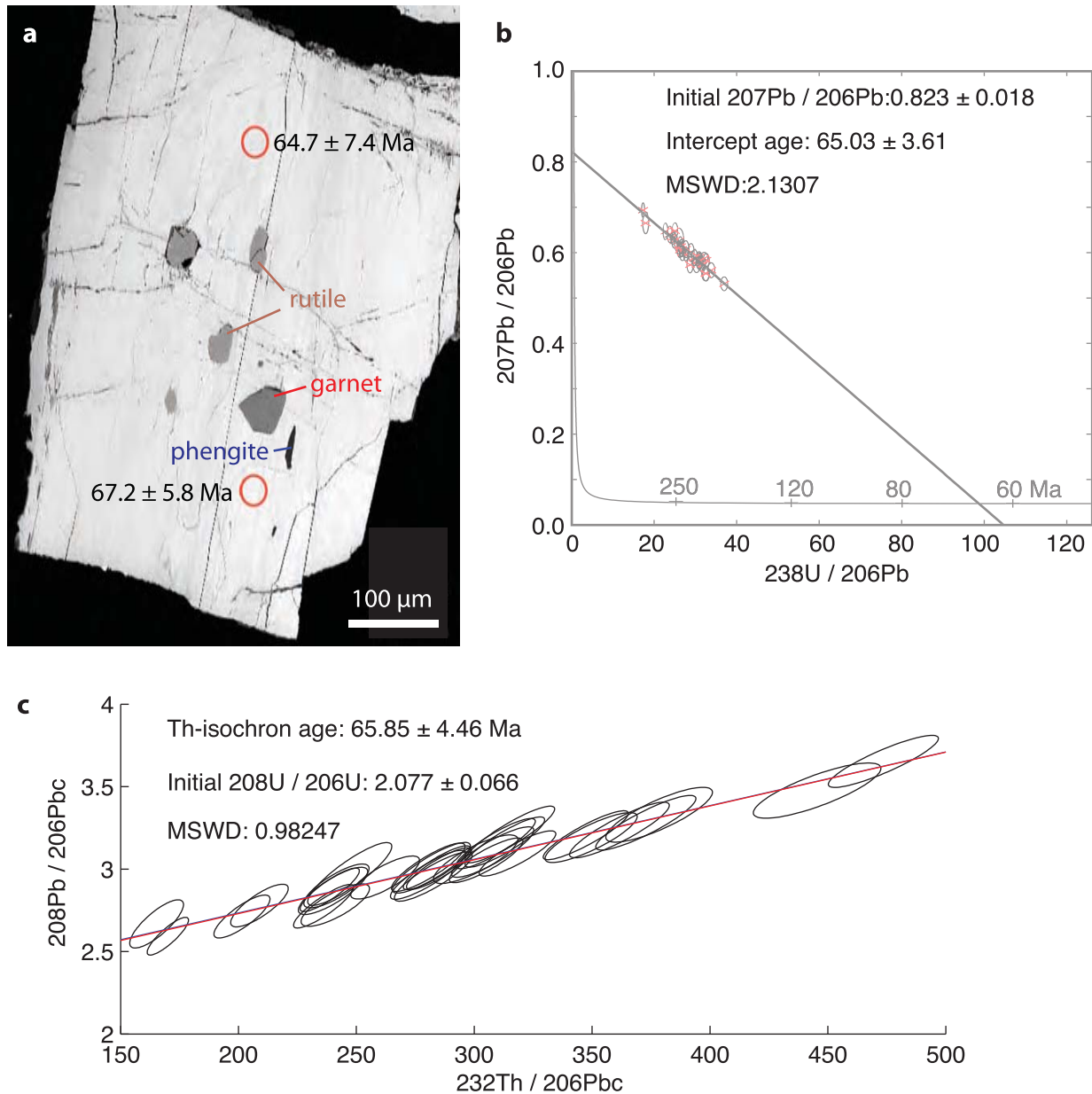


Figure 5. Allanite age dating. Data for sample FG1315. (a) Chemically uniform prism of metamorphic allanite ($\text{Th}/\text{U} = 7.4 \pm 1.5$) containing inclusions of garnet (stage-2 or stage-3), rutile, and phengite (with same composition as in the rock matrix). Thirty-two spot analyses (in situ LA-ICP-MS data, laser \varnothing 32 μm) yield concordant $^{208}\text{Pb}/^{232}\text{Th}$ and $^{206}\text{Pb}/^{238}\text{U}$ ages; analytical error of spot analyses is 2SD. (b) Tera-Wasserburg plot of all data define an intercept age: 65.0 ± 3.6 Ma, in good agreement with Figure 5c, the Th/Pb isochron age: 65.9 ± 4.5 Ma. Red circles mark laser spots. Complete data in supporting information supporting Tables S5 and S6.

200°C lower; hence, the garnet HT cores are clearly pre-Alpine. Earlier studies (Lardeaux & Spalla, 1991; Zucali et al., 2002) of the Sesia Zone reported similar PT data for this early HT stage.

For each of the subsequent stages of garnet growth, the observed corrosion features were taken to indicate that a free aqueous fluid had been present, hence at each stage of modeling we added sufficient H_2O to the bulk composition for the final assemblages to be fluid-saturated. In order to obtain garnet compositions matching those analyzed, we accounted for the nonreactive portion of garnet (Lanari & Engi, 2017). Once the locally effective bulk (LEB) composition was optimized, the predicted composition for each stage matched the observed one very closely (supporting information Table S4), thus lending credibility to the approach and to the thermobarometric results. It is noteworthy that our initial assumption of a model

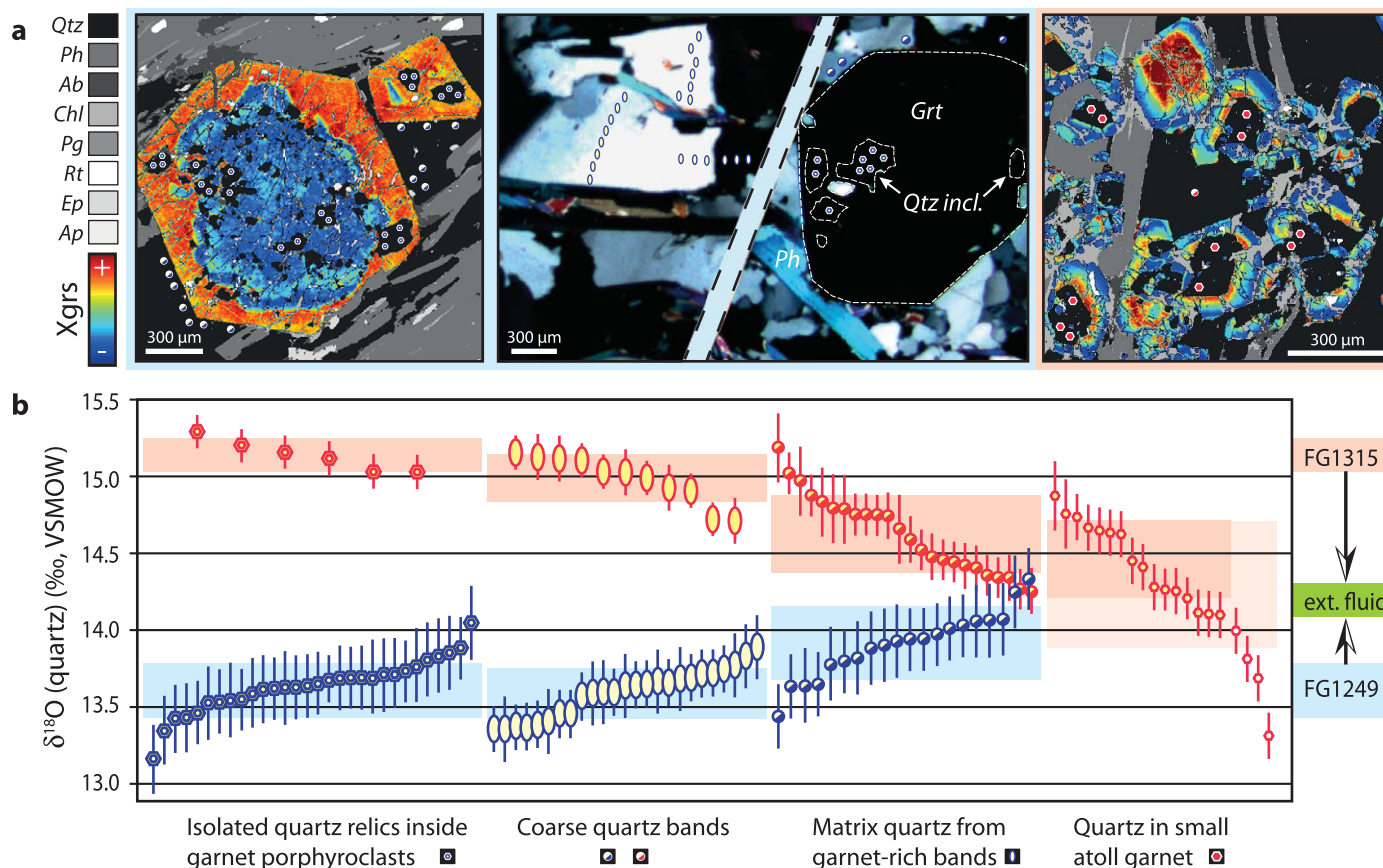


Figure 6. Oxygen isotopic data for quartz from textural domains of different age. (a) Photomicrograph shows the position of four types of quartz domains; these were subsequently extracted for oxygen isotopic analysis. Photos taken with crossed-polarizers were overlain with images showing Ca-zoning in garnet (X_{Grs} : mole fraction of grossular component). Single analytical spots are shown in their original context, with their texturally identified (relative) age indicated by symbols: white hexagons (oldest), ellipses (second), half-filled circles (third), and red circles (youngest). (b) Data of $\delta^{18}\text{O}$ in quartz are arranged for two samples in the relative age sequence, from earliest to latest, as identified prior to analysis. The data for each sample show very small but systematic variations, indicating minor heterogeneity in $\delta^{18}\text{O}$ at grain scale. Values from left (oldest) to right (youngest) indicate a trend, with average values (colored bands indicate $\pm 1\text{SD}$ around the mean) showing a decrease for one sample (FG1315), but an increase for the other one (FG1249). Note that data within each group are ordered according to their $\delta^{18}\text{O}$ -values, not spatial proximity, to emphasize the trend shown by the medians. These data are consistent with oxygen isotopic exchange of quartz with an externally derived fluid. Raw data in supporting information Table S4.

system closed to all components, apart from H_2O , proved sufficient to obtain such a close match, with sub-equal residuals for all garnet components, even for the earliest (core) garnet. This indicates that metasomatism was very minor, and the fluid hydrating the rocks probably was of a typical crustal composition (high $a_{\text{H}_2\text{O}}$). Our oxygen isotope data from quartz are in line with this inference.

The results show prograde HP conditions, from rim-1 to rim-3 (1.5 \rightarrow 1.8 GPa, 650 \rightarrow 670°C), thus a sequence reflecting subduction. Stage-3 is the only one for which the model predictions can be compared with the complete eclogite facies assemblage observed in the sample. The agreement is excellent, including the compositions of the solution phases (garnet, phengite, paragonite) coexisting at equilibrium.

Using our thermodynamic modeling approach, it was thus possible to confirm the petrographic evidence of repeated stages of garnet cannibalism and to quantify its extent. (The term cannibalism is used to indicate a complex process that probably involved local dissolution and reprecipitation of the same mineral phase.) We distinguish three stages in the Alpine HP evolution. In each of these, hydration combined with partial resorption of earlier formed garnet, lead to the formation of a new garnet generation. Though the range of PT data obtained for these three stages is fairly small, we stress that no satisfactory model was obtained for a single set of average PT conditions. The PT differences between at least two of the three stages are considered significant, i.e., stage-1 certainly differs from stage-2. The succession found here is similar to PT

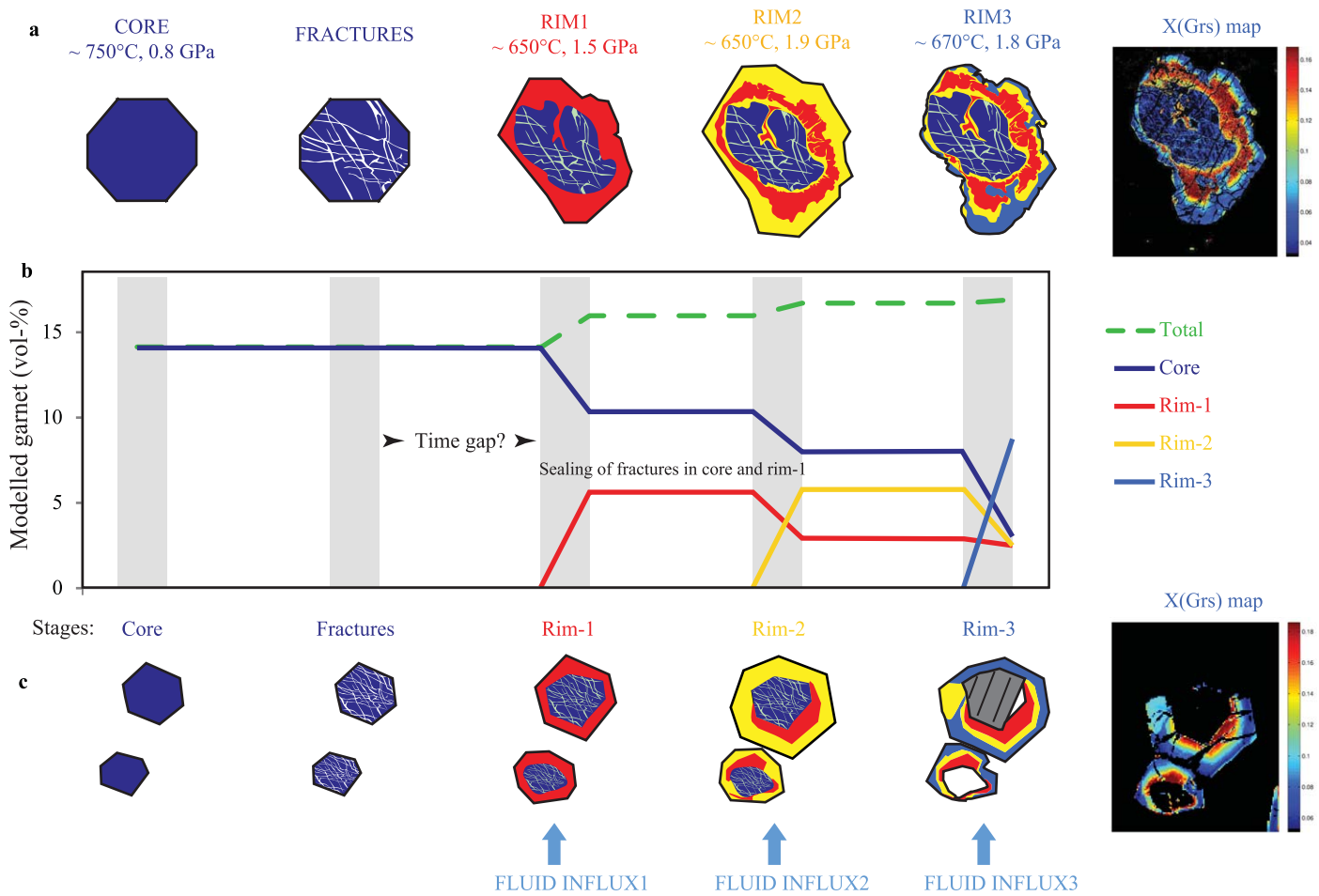


Figure 7. Stages of garnet evolution. Based on data in sample FG1315 (Figure 3). (a) Morphology and chemical zoning preserved, schematic stages leading to the observed grossular concentration (right: X-ray map for Ca). (b) Relative temporal sequence from Permian core to Alpine rims (65 Ma for rim-2 or rim-3, Figure 5). Thermodynamic modeling of this sample indicates three stages of partial resorption, each of them followed by new garnet growth. (c) Zoning of atoll garnet: the small pre-Alpine core was completely resorbed and replaced mostly by phengite (grey) and quartz (white).

paths determined in other studies (e.g., Giuntoli et al., 2018; Regis et al., 2014; Rubatto et al., 2011; Zucali, 2011) of the area sampled.

Taken together, textural, mineral chemical, isotopic evidence, and thermodynamic modeling from garnet, quartz, and zircon all point to a polyphase evolution of the samples: After pre-Alpine *HT* metamorphism followed intense brittle deformation and several phases of hydration, which triggered mineral growth and repeated chemical resorption at grain scale. This intense hydration, dated at ~65 Ma, pervasively transformed the dry Permian basement rocks to eclogitic micaschists.

5. Discussion

5.1. Fracturing and Hydration in the Subduction Channel

Eclogitic micaschists are the dominant lithotype in the Sesia Zone. The characteristics documented in section 3.1 indicate that the micaschists originally derived from clastic sediments (Figure 1) containing fragments of mafic intrusives. Closely analogous rock suites occur not only in cognate tectonic units of the Western Alps, but also in the Ivrea Zone (Handy et al., 1999). Whereas the Ivrea Zone retains pre-Alpine high-temperature characteristics, the units in the Western Alps were all subducted, intensely deformed and metamorphosed at HP. On comparing the suites, metapelites in the Ivrea samples are found to be largely dehydrated (to <0.5 wt % H₂O in granulite facies samples), whereas HP samples of the Western Alps show ~1.5% H₂O at blueschist and ~2.0% H₂O at eclogite facies conditions (Figure 2). The Ivrea values imply that 80–90% of the original water in the protolith sediments (pelites: 4.5–7 wt % H₂O, Nicholls & Loring, 1962)

was lost in the course of high-temperature metamorphism. Provided the Ivrea metapelites are valid proxies, the HP derivatives must have experienced pervasive rehydration. To determine at what stage this occurred, the network of healed hairline fractures preserved in garnet deserves closer scrutiny: Cores show very intense fracturing; rim-1 shows fewer fractures, and these are less sharp and pervasive; rim-3 shows no fractures. All fractures were healed by thin garnet seams that correspond in composition to rim-2, some of them possibly rim-1. We infer that repeated, intense brittle deformation initiated and subsequently—possibly after a temporal gap (Figure 7)—allowed fluid access and garnet cannibalism, which occurred during subduction. Partial hydration associated with Permo-Mesozoic extension is not excluded but in the Sesia Zone there is little evidence for it. Some garnet is porphyroclastic, but many of the densely fractured grains remained intact, showing no displacement or shear. If brittle deformation during the Permo-Mesozoic extension had affected the granulites, then hydration at low pressures and temperatures should have transformed the dry protoliths to micaschists, and chlorite would most likely have formed at the expense of garnet, notably along its fractures. During subduction, it seems inevitable that such mechanically weak material would have been sheared, and one could scarcely expect the intact shape of original garnet grains preserved. Instead, we consistently find hairline fractures that were but very locally (at μm -scale; Figure 3) lined by seams of a Ca-enriched variety, which clearly is of HP origin. To account for these observations, we propose that intense brittle deformation affected the granulite precursors in the Alpine subduction channel, likely associated with seismic failure, which caused disruption but minimal displacement, enhancing permeability and hence fluid access. The ensuing hydration reactions, e.g., of feldspars to white micas, are strongly exothermic, thus causing expansion of hydrous fluid during percolation. Such thermally induced crack propagation and hydrofracturing probably facilitated pervasive hydration. Garnet fracturing and alteration attributed to seismic failure at eclogite facies conditions has been reported from Western Norway (Austrheim et al., 1996, 2017), but there it is closely linked to localized shear planes and pseudotachylites, and hydration is far more limited than in the Sesia Zone. In both cases, fracturing affected rather dry protoliths, but in the Western Gneiss Region a substantial portion of these preserve metastable HT assemblages (Lund & Austrheim, 2003), whereas in the Sesia Zone they were pervasively hydrated and converted to eclogitic micaschists. This may explain the absence of eclogitic pseudotachylites or cataclasites, since such highly reactive rocks would readily equilibrate when hydrated.

We note that the metasediments, inasmuch as they entered the subduction channel as granulites and upper amphibolite facies rocks, were not sources but sinks of hydrous fluid upon descent. The observed HP assemblages imply an uptake of ~ 1.5 wt % H_2O during subduction. As fluid flow in Alpine-type settings is thought to be dominantly subduction-parallel (Angiboust et al., 2012), the length scale of the flow is quite uncertain. For this reason, it would be adventurous to translate this fluid intake into an integrated fluid flux (Ferry & Dipple, 1991). The original source of the HP fluids responsible for the rehydration is equally speculative, but we note that subduction starting in the mid-Cretaceous has been invoked (Dal Piaz et al., 2003), and sediments accreted along the internal Adriatic margin (e.g., Canavese; Beltrando et al., 2014) would likely have been dehydrated during subduction, as would previously hydrated oceanic crust and serpentinized parts of the Adriatic mantle (Schmid et al., 2017).

Additional hydration, especially associated with exhumation-related regional shear zones, is well known in some parts of the Sesia Zone. This overprint may be linked to interaction of HP rocks with fluids derived by later dehydration of oceanic rocks (Konrad-Schmolke et al., 2011a). Neither the oxygen isotopic data nor the ages we determined suggest that such fluids substantially modified our samples. The pervasive imprint we dated in the Sesia eclogitic micaschists (~ 65 Ma) is much older than the HP rocks exhumed with parts of the oceanic slab (mostly 50–40 Ma in Piemonte-Liguria). We did not observe metasomatic effects typical of interaction with oceanic fluids, and retrogression is very minor. Our samples show that conversion of granulites to eclogitic micaschists occurred during subduction. Contrary to other interpretations (Konrad-Schmolke et al., 2011a), our data show that most of the rehydration preceded exhumation (see also Giuntoli et al., 2018).

5.2. Implications on Tectonics and Recycling of Continental Crust

Tectonic fragments in HP terrains (e.g., Norwegian Caledonides, Zambia) show that lower crustal rocks are not readily transformed to eclogite facies, except where deformation and fluid flow (Austrheim, 1987; Austrheim et al., 1997; John & Schenk, 2003) reduce kinetic barriers (Krabbendam et al., 2000; Wain et al., 2001). Densification of continental units in Western Norway is mostly limited to shear zones, with large volumes of

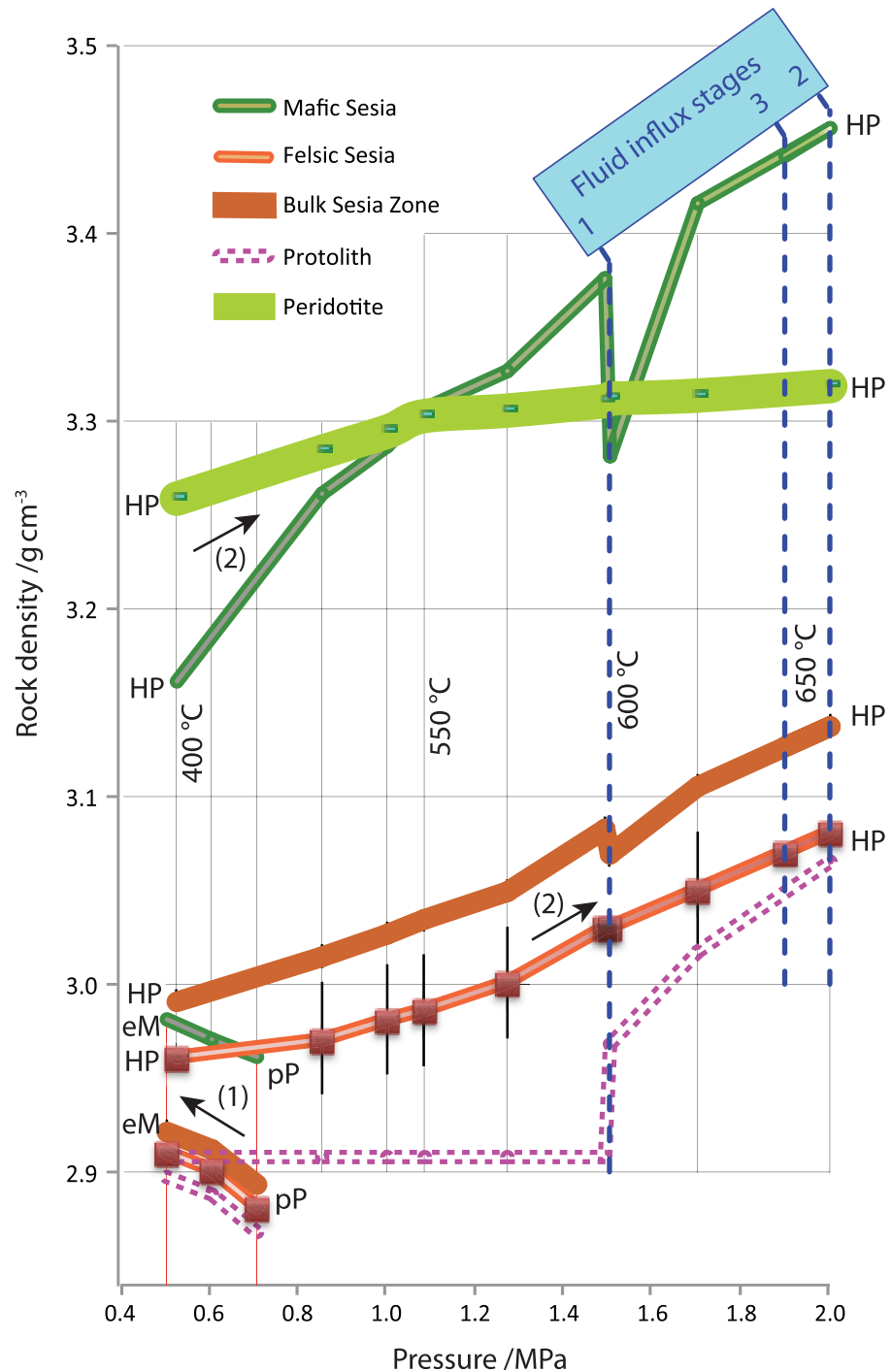


Figure 8. Density of rocks along post-Permian and late Cretaceous geothermal gradients. Density modeled (using Theriak; de Capitani & Petrakakis, 2010) for assemblages evolving in two steps: Arrow (1) post-Permian extensional exhumation, from peak Permian (pP) to early Mesozoic (eM) *PT* conditions, i.e., 0.7 → 0.5 GPa, 750 → 500°C; Arrow (2) Alpine subduction (HP): 0.5 → 2 GPa, 400 → 650°C. P-T conditions after Lanari et al. (2017). Fluid-starved conditions were assumed from Permian to early Mesozoic. During prograde Alpine evolution, hydrous fluid was added in three pulses (at 1.5, 1.9, and 1.8 GPa, as shown in Figure 7). For mafic rocks, the first hydration pulse lead to formation of sodic amphibole, whence the density drop. Data sets are based on representative rock compositions: For *Mafic Sesia* sample MK58 (Konrad-Schmolke, 2006) was used; for *Felsic Sesia* FG1315 (supporting information Table S1) was used; error bars denote ±1% relative uncertainty between data sets; *Bulk Sesia* denotes estimated overall abundances (85% felsic; 15% mafic) in the Sesia Zone; *Protolith* assumes that the Permian *HT* assemblage survived metastably until a first pulse of fluid; *Peridotite* is based on a mix of 75% chlorite harzburgite, 25% lherzolite (density from Walsh & Hacker, 2004).

granulites surviving metastably, despite subduction to >60 km depth (Austrheim, 1987; Bjørnerud et al., 2002; Wain et al., 2001). The IC in the central Sesia Zone, where the subduction depth was similar, was almost completely eclogitized (Compagnoni, 1977). We attribute this striking difference to major differences in deformation and fluid flow: In Norway, strain is mostly localized in shear zones, where fluid flow is channeled; in Sesia intense fracturing permitted fluid percolation at grain scale.

Such differences have significant consequences on density evolution and potentially on tectonics. Numerical models simulating tectonic flow in a subduction channel (Gerya et al., 2002; Warren et al., 2008) find that the buoyancy of fragments is decisive. However, which fragments descend into the mantle or escape upward along the subduction interface, is unclear. Importantly, the Earth's crust is compositionally differentiated, and this has bearings on continental recycling and mantle metasomatism.

A comprehensive plate-tectonic reconstruction (Handy et al., 2010) links the HP units exposed in the Western Alps, including the Sesia Zone, with a tomographically evident (Kissling et al., 2006) slab remnant, some 1,000 km long and at ~550 km depth (Figures 13 and 15 in Handy et al., 2010). Unfortunately, seismic imaging cannot resolve sufficient local density contrast to infer what rock types may constitute such a subduction graveyard. Density modeling is useful, however, to explore relative buoyancy of a realistic range of rock compositions and to take into account the evidently variable effects of fluids. Because the Ivrea Zone exposes a cross section through the middle and lower continental crust, fragments of which had been integrated into the subducted slab, the lithotypes involved are known. Details of our model are given in supporting information. Results shown in Figure 8 assumed zero porosity and thus should be regarded as upper limits to the rock densities.

For the felsic lithotypes modeled, the density evolution during PT increase shows transient effects of hydration where dry precursors are converted to fully hydrated eclogite assemblages. The effect is much more pronounced for mafic rocks (due to stabilization of epidote and amphibole), provided equilibrium assemblages did form at temperatures below ~600°C. If so, the first stage of fluid influx may temporarily have inverted their buoyancy relative to mantle peridotite (at depths of 40–50 km). In any case, slab parts that reach 50 km depth and contain at least 70% mafic lithotypes, even if hydrated during subduction, are expected to keep descending into the upper mantle. The tomographically evident fragments in the mantle transition zone are likely to be mostly mafic in composition and may include only a minor fraction of highly differentiated rocks. Conversely, density modeling confirms that (lower crustal) portions of the descending slab similar in composition to the Sesia Zone, i.e., dominated by felsic lithotypes, remained quite positively buoyant relative to the mantle, which facilitated their return to the surface. If the rheology in the subduction channel permits changes in buoyancy to drive tectonic mixing, then fragments of mostly felsic composition should recycle within the crust, even if completely converted to dense HP assemblages. Where deformation and fluid flow are mostly localized, such densification is unlikely, and fragments of dominantly mafic composition, once foundered, are likely to escape upward as well. Our density modeling indicates that, in order to exert slab-pull into the upper mantle, even mafic crustal rocks first have to be largely transformed to eclogite (as proposed for Western Norway; Austrheim et al., 1997; Bjørnerud & Austrheim, 2004).

6. Conclusions

This case study, conducted in the central Sesia Zone, leads to conclusions of general interest for continental subduction settings, notably including the following:

1. Upon subduction, granulites and similarly dry rocks of the lower continental crust can act as *fluid sinks*, with hydrous fluid entering through a network of brittle fractures, which likely resulted from seismic failure.
2. Interaction with hydrous fluids causes *extensive rehydration* in subducted fragments of lower crust: Irreversible reactions replace HT minerals by dense, hydrous HP assemblages (producing, e.g., eclogitic micaschists).
3. Density modeling indicates that the rehydration-induced *densification* in the subduction channel may be a critical switch for the *dynamic separation* of continental fragments, with dense rock types feeding a subduction graveyard, whereas light ones return upward and may feed an orogen. If the exhumed Sesia eclogite terrain indeed is linked to the tomographically evident high-density remnants (at ~550 km, in

the Mantle transition zone) beneath the Alps, these would have to be dominated by mafic lithotypes, mostly eclogites.

4. In Sesia samples, we discovered that *refractory mineral relics*, notably garnet, preserve a detailed record of cannibalism (stepwise partial autoreplacement). We developed a quantitative *model* of the successive fluid-rock interactions. Combined with U-Th-Pb *petrochronology* (on allanite and zircon) this allowed us to extract the P-T-t conditions at which the transformations occurred.
5. This study emphasizes important *connections* between (seismically induced?) brittle deformation, the percolation of hydrous fluids through lower crustal fragments, and the mineral reactions thus induced. More work is needed to constrain the *origin and chemistry of external fluids* that can cause rehydration in continental subduction zones.

Acknowledgments

We thank R. Compagnoni, D. Rubatto, J. Hermann, T. Pettke, L. Baumgartner, E. Kissling, C. de Capitani, and A. J. Smye for helpful input and fruitful discussions. The Swiss National Science Foundation (grant 200020-146175) supported this research. Constructive reviews by H. Stünitz and G. Mohn are gratefully acknowledged, as is the editorial handling by T. Becker. All analytical data (supporting information Tables S1, S3, S5, and S6) are available as Excel files on the EarthChem Library (<https://doi.org/10.1594/IEDA/100745>). Author contributions: M.E. conceived and supervised the research. F.G. did the field work and petrological analysis with guidance from P.L. and M.E.; M.B., B.K., P.L., and A.-S.B. measured isotopic data. P.L., F.G., and M.E. did the modeling. M.E. wrote the paper, with contributions from all coauthors. The authors declare no competing financial interests.

References

- Abers, G. A., Nakajima, J., van Keken, P. E., Kita, S., & Hacker, B. R. (2013). Thermal-petrological controls on the location of earthquakes within subducting plates. *Earth and Planetary Science Letters*, 369–370, 178–187. <https://doi.org/10.1016/j.epsl.2013.03.022>
- Angiboust, S., Wolf, S., Burro, E., Agard, P., & Yamato, P. (2012). Effect of fluid circulation on subduction interface tectonic processes: Insights from thermo-mechanical numerical modelling. *Earth and Planetary Science Letters*, 357–358, 238–248. <https://doi.org/10.1016/j.epsl.2012.09.012>
- Angiboust, S., Yamato, P., Hertgen, S., Hyppolito, T., Bebout, G. E., & Morales, L. (2017). Fluid pathways and high-P metasomatism in a subducted continental slice (Mt. Emilius klippe, W. Alps). *Journal of Metamorphic Geology*, 35(5), 471–492. <https://doi.org/10.1111/jmg.12241>
- Austrheim, H. (1987). Eclogitization of lower crustal granulites by fluid migration through shear zones. *Earth and Planetary Science Letters*, 81(2–3), 221–232. [https://doi.org/10.1016/0012-821X\(87\)90158-0](https://doi.org/10.1016/0012-821X(87)90158-0)
- Austrheim, H., Dunkel, K. G., Plümper, O., Ildefonse, B., Liu, Y., & Jamtveit, B. (2017). Fragmentation of wall rock garnets during deep crustal earthquakes. *Science Advances*, 3(2), e1602067. <https://doi.org/10.1126/sciadv.1602067>
- Austrheim, H., Erambert, M., & Boundy, T. M. (1996). Garnets recording deep crustal earthquakes. *Earth and Planetary Science Letters*, 139(1–2), 223–238. [https://doi.org/10.1016/0012-821X\(95\)00232-2](https://doi.org/10.1016/0012-821X(95)00232-2)
- Austrheim, H., Erambert, M., & Engvik, A. K. (1997). Processing of crust in the root of the Caledonid continental collision zone: The role of eclogitization. *Tectonophysics*, 273, 129–153.
- Barcheck, C. G., Wiens, D. A., van Keken, P. E., & Hacker, B. R. (2012). The relationship of intermediate- and deep-focus seismicity to the hydration and dehydration of subducting slabs. *Earth and Planetary Science Letters*, 349–350, 153–160. <https://doi.org/10.1016/j.epsl.2012.06.055>
- Beltrando, M., Manatschal, G., Mohn, G., Dal Piaz, G. V., Vitale Brovarone, A., & Masini, E. (2014). Recognizing remnants of magma-poor rifted margins in high-pressure orogenic belts: The Alpine case study. *Earth-Science Reviews*, 131, 88–115. <https://doi.org/j.earscirev.2014.01.001>
- Beltrando, M., Rubatto, D., & Manatschal, G. (2010). From passive margins to orogens: The link between ocean-continent transition zones and (ultra)high-pressure metamorphism. *Geology*, 38(6), 559–562. <https://doi.org/10.1130/G30768.1>
- Bjørnerud, M. G., & Austrheim, H. (2004). Inhibited eclogite formation: The key to the rapid growth of strong and buoyant Archean continental crust. *Geology*, 32(9), 765–768. <https://doi.org/10.1130/G20590.1>
- Bjørnerud, M. G., Austrheim, H., & Lund, M. G. (2002). Processes leading to eclogitization (densification) of subducted and tectonically buried crust. *Journal of Geophysical Research*, 107(B10), 2252. <https://doi.org/10.1029/2001JB000527>
- Burn, M. (2012). *Evolution of the Monte Emilius Klippe (Val d'Aosta, Italy)* (MSc thesis), Bern, Switzerland: University of Bern.
- Burn, M., Lanari, P., Pettke, T., & Engi, M. (2017). Non-matrix-matched standardisation in LA-ICP-MS analysis: General approach and application to allanite Th-U-Pb age-dating. *Journal of Analytical Atomic Spectrometry*, 32(7), 1359–1377. <https://doi.org/10.1039/C7JA00095B>
- Chenin, P., Manatschal, G., Picazo, S., Müntener, O., Karner, G., Johnson, C. M., et al. (2017). Influence of the architecture of magma-poor hyperextended rifted margins on orogens produced by the closure of narrow versus wide oceans. *Geosphere*, 13(2), 559–576. <https://doi.org/10.1130/ges01363.1>
- Clayton, R. N., O'Neil, J. R., & Mayeda, T. K. (1972). Oxygen isotope exchange between quartz and water. *Journal of Geophysical Research*, 77(17), 3057–3067. <https://doi.org/10.1029/JB077i017p03057>
- Compagnoni, R. (1977). The Sesia-Lanzo Zone: High pressure-low temperature metamorphism in the Austroalpine continental margin. *Rendiconti della Società Italiana di Mineralogia e Petrologia*, 33, 335–375.
- Dal Piaz, G. V. (1999). The Austroalpine-Piedmont nappe stack and the puzzle of the Alpine Tethys. *Memorie di Scienze Geologiche*, 51(1), 155–176.
- Dal Piaz, G. V., Bistacchi, A., & Massironi, M. (2003). Geological outline of the Alps. *Episodes*, 26(3), 175–180.
- de Capitani, C., & Petrakakis, K. (2010). The computation of equilibrium assemblage diagrams with Theriak/Domino software. *American Mineralogist*, 95(7), 1006–1016. <https://doi.org/10.2138/am.2010.3354>
- Diehl, E. A., Masson, R., & Stutz, A. H. (1952). Contributo alla conoscenza del ricoprimento della Dent Blanche. *Memorie degli Istituti di Geologia e Mineralogia dell'Università di Padova*, 17, 1–52.
- Engi, M. (2017). Petrochronology based on REE-minerals: Monazite, allanite, xenotime, apatite. *Reviews in Mineralogy and Geochemistry*, 83, 365–418. <https://doi.org/10.2138/rmg.2017.83.12>
- Ferry, J. M., & Dipple, G. M. (1991). Fluid flow, mineral reactions, and metasomatism. *Geology*, 19, 211–214.
- Gaidies, F., de Capitani, C., & Abart, R. (2008). THERIA_G: A software program to numerically model prograde garnet growth. *Contributions to Mineralogy and Petrology*, 155(5), 657–671. <https://doi.org/10.1007/s00410-007-0263-z>
- Geisler, T., Schaltegger, U., & Tomaschek, F. (2007). Re-equilibration of zircon in aqueous fluids and melts. *Elements*, 3, 43–50.
- Gerya, T. V., Stöckhert, B., & Perchuk, A. L. (2002). Exhumation of high-pressure metamorphic rocks in a subduction channel: A numerical simulation. *Tectonics*, 21(6), 1056. <https://doi.org/10.1029/2002TC001406>
- Giuntoli, F. (2016). *Assembly of continental fragments during subduction at HP: Metamorphic history of the central Sesia Zone (NW Alps)* (PhD thesis). Bern, Switzerland: University of Bern.

- Giuntoli, F., & Engi, M. (2016). Internal geometry of the central Sesia Zone (Aosta Valley, Italy): HP tectonic assembly of continental slices. *Swiss Journal of Geosciences*, 110, 1–27. <https://doi.org/10.1007/s00015-016-0225-4>
- Giuntoli, F., Lanari, P., Burn, M., Kunz, B., & Engi, M. (2018). Deeply subducted continental fragments: II. Insight from petrochronology in the central Sesia Zone (Western Italian Alps). *Solid Earth*, 9, 191–222. <https://doi.org/10.5194/se-9-191-2018>
- Giuntoli, F., Lanari, P., & Engi, M. (2018). Deeply subducted continental fragments: I. Fracturing, dissolution-precipitation and diffusion processes recorded by garnet textures of the central Sesia Zone (Western Italian Alps). *Solid Earth*, 9, 167–189. <https://doi.org/10.5194/se-9-167-2018>
- Gregory, C., Rubatto, D., Hermann, J., Berger, A., & Engi, M. (2012). Allanite behaviour during incipient melting in the southern Central Alps. *Geochimica et Cosmochimica Acta*, 84, 433–458. <https://doi.org/10.1016/j.gca.2012.01.020>
- Hacker, B. R., Kelemen, P. B., & Behn, M. D. (2011). Differentiation of the continental crust by relamination. *Earth and Planetary Science Letters*, 307(3–4), 501–516. <https://doi.org/10.1016/j.epsl.2011.05.024>
- Handy, M. R., Franz, L., Heller, F., Janott, B., & Zurrbruggen, R. (1999). Multistage accretion and exhumation of the continental crust (Ivrea crustal section, Italy and Switzerland). *Tectonics*, 18(6), 1154–1177. <https://doi.org/10.1029/1999TC900034>
- Handy, M. R., Schmid, S. M., Bousquet, R., Kissling, E., & Bernoulli, D. (2010). Reconciling plate-tectonic reconstructions of Alpine Tethys with the geological-geophysical record of spreading and subduction in the Alps. *Earth-Science Reviews*, 102(3–4), 121–158. <https://doi.org/10.1016/j.earscirev.2010.06.002>
- Hermann, J., & Rubatto, D. (2003). Relating zircon and monazite domains to garnet growth zones: Age and duration of granulite facies metamorphism in the Val Malenco lower crust. *Journal of Metamorphic Geology*, 21(9), 833–852. <https://doi.org/10.1046/j.1525-1314.2003.00484.x>
- Hetényi, G., Cattin, R., Brunet, F., Bollinger, L., Vergne, J., Nábělek, J. L., et al. (2007). Density distribution of the India plate beneath the Tibetan plateau: Geophysical and petrological constraints on the kinetics of lower-crustal eclogitization. *Earth and Planetary Science Letters*, 264(1–2), 226–244. <https://doi.org/10.1016/j.epsl.2007.09.036>
- Höpfer, N. (1997). *Sedimentäre Abfolge und alpine Überprägung der Permotriassischen Roisan Zone (südliche Austroalpine Dent Blanche Decke, italienische Westalpen)* (PhD thesis). Wiehl, Germany: Universität Bonn.
- Janots, E., Engi, M., Rubatto, D., Berger, A., Gregory, C., & Rahn, M. (2009). Metamorphic rates in collisional orogeny from in situ allanite and monazite dating. *Geology*, 37(1), 11–14. <https://doi.org/10.1130/G25192A.1>
- John, T., & Schenk, V. (2003). Partial eclogitisation of gabbroic rocks in a late Precambrian subduction zone (Zambia): Prograde metamorphism triggered by fluid infiltration. *Contributions to Mineralogy and Petrology*, 146(2), 174–191. <https://doi.org/10.1007/s00410-003-0492-8>
- Kissling, E., Schmid, S. M., Lippitsch, R., Ansoerge, J., & Fügenschuh, B. (2006). Lithosphere structure and tectonic evolution of the Alpine arc: New evidence from high-resolution teleseismic tomography. *Geological Society, London, Memoirs*, 32(1), 129–145. <https://doi.org/10.1144/GSL.MEM.2006.032.01.08>
- Konrad-Schmolke, M. (2006). *Insights into subduction and exhumation mechanisms of continental crust—An example from the Sesia zone (Western Alps)* (PhD thesis). Berlin, Germany: Free University of Berlin.
- Konrad-Schmolke, M., O'Brien, P. J., & Zack, T. (2011a). Fluid migration above a subducted slab—Constraints on amount, pathways and major element mobility from partially overprinted eclogite-facies rocks (Sesia Zone, Western Alps). *Journal of Petrology*, 52(3), 457–486. <https://doi.org/10.1093/petrology/egq087>
- Konrad-Schmolke, M., Zack, T., O'Brien, P. J., & Barth, M. (2011b). Fluid migration above a subducted slab—Thermodynamic and trace element modelling of fluid-rock interaction in partially overprinted eclogite-facies rocks (Sesia Zone, Western Alps). *Earth and Planetary Science Letters*, 311(3–4), 287–298. <https://doi.org/10.1016/j.epsl.2011.09.025>
- Krabbendam, M., Wain, A. L., & Andersen, T. B. (2000). Pre-Caledonian granulite and gabbro enclaves in the Western Gneiss Region, Norway: Indications of incomplete transition at high pressure. *Geological Magazine*, 137(3), 235–255.
- Labrousse, L., Duret, T., & Gerya, T. (2015). H₂O-fluid-saturated melting of subducted continental crust facilitates exhumation of ultrahigh-pressure rocks in continental subduction zones. *Earth and Planetary Science Letters*, 428, 151–161. <https://doi.org/10.1016/j.epsl.2015.06.016>
- Lanari, P., & Engi, M. (2017). Local bulk composition effects on metamorphic mineral assemblages. *Reviews in Mineralogy and Geochemistry*, 83, 55–102. <https://doi.org/10.2138/rmg.2017.83.3>
- Lanari, P., Giuntoli, F., Louri, C., Burn, M., & Engi, M. (2017). An inverse modeling approach to obtain P-T conditions of metamorphic stages involving garnet growth and resorption. *European Journal of Mineralogy*, 29(2), 181–199. <https://doi.org/10.1127/ejm/2017/0029-2597>
- Lanari, P., Vidal, O., De Andrade, V., Dubacq, B., Lewin, E., Grosch, E. G., et al. (2014). XMapTools a Matlab®-based graphic user interface for microprobe quantified image processing. *Computers & Geosciences*, 62, 227–240. <https://doi.org/10.1016/j.cageo.2013.08.010>
- Lardeaux, J. M., & Spalla, M. I. (1991). From granulites to eclogites in the Sesia zone (Italian Western Alps): A record of the opening and closure of the Piedmont Ocean. *Journal of Metamorphic Geology*, 9, 35–59.
- Li, Y. L., Zheng, Y. F., Fu, B., Zhou, J. B., & Wei, C. S. (2001). Oxygen isotope composition of quartz-vein in ultrahigh-pressure eclogite from Dabieshan and implications for transport of high-pressure metamorphic fluid. *Physics and Chemistry of the Earth A*, 26(9–10), 695–704. [https://doi.org/10.1016/S1464-1895\(01\)00120-X](https://doi.org/10.1016/S1464-1895(01)00120-X)
- Lippitsch, R., Kissling, E., & Ansoerge, J. (2003). Upper mantle structure beneath the Alpine orogen from high-resolution teleseismic tomography. *Journal of Geophysical Research*, 108(B8), 2376. <https://doi.org/10.1029/2002JB002016>
- Lund, M. G., & Austrheim, H. (2003). High-pressure metamorphism and deep-crustal seismicity: Evidence from contemporaneous formation of pseudotachylytes and eclogite facies coronas. *Tectonophysics*, 372(1–2), 59–83. [https://doi.org/10.1016/S0040-1951\(03\)00232-4](https://doi.org/10.1016/S0040-1951(03)00232-4)
- Manatschal, G. (2004). New models for evolution of magma-poor rifted margins based on a review of data and concepts from West Iberia and the Alps. *International Journal of Earth Sciences*, 93(3), 432–466. <https://doi.org/10.1007/s00531-004-0394-7>
- Manzotti, P., Ballèvre, M., Zucali, M., Robyr, M., & Engi, M. (2014). The tectonometamorphic evolution of the Sesia-Dent Blanche nappes (internal Western Alps): Review and synthesis. *Swiss Journal of Geosciences*, 207, 107(2–3), 309–336. <https://doi.org/10.1007/s00015-014-0172-x>
- Manzotti, P., Zucali, M., Ballèvre, M., Robyr, M., & Engi, M. (2014). Geometry and kinematics of the Roisan-Cignana Shear Zone, and the orogenic evolution of the Dent Blanche Tectonic System (Western Alps). *Swiss Journal of Geosciences*, 107(1), 23–48. <https://doi.org/10.1007/s00015-014-0157-9>
- Matthews, A., & Beckinsale, R. D. (1979). Oxygen isotope equilibration systematics between quartz and water. *American Mineralogist*, 64(2), 232–240.
- Mohn, G., Manatschal, G., Beltrando, M., & Hauptert, I. (2014). The role of rift-inherited hyper-extension in Alpine-type orogens. *Terra Nova*, 26(5), 347–353. <https://doi.org/10.1111/ter.12104>
- Nesbitt, H. W., & Young, G. M. (1982). Early Proterozoic climates and plate motions inferred from major element chemistry of lites. *Nature*, 299(5885), 715–717. <https://doi.org/10.1038/299715a0>

- Nicholls, G. D., & Loring, D. H. (1962). The geochemistry of some British carboniferous sediments. *Geochimica et Cosmochimica Acta*, 26(2), 181–223. [https://doi.org/10.1016/0016-7037\(62\)90012-1](https://doi.org/10.1016/0016-7037(62)90012-1)
- Pennacchioni, G. (1996). Progressive eclogitization under fluid-present conditions of pre-Alpine mafic granulites in the Austroalpine Mt Emilius Klippe (Italian western Alps). *Journal of Structural Geology*, 18(5), 549–561.
- Redler, C. (2011). *Granulite facies metamorphism and partial melting processes in the Ivrea zone, Northern Italy* (PhD thesis). Mainz, Germany: University of Mainz.
- Regis, D. (2012). *High-pressure evolution in the Sesia terrane (Italian Western Alps)* (PhD thesis). Bern, Switzerland: University of Bern.
- Regis, D., Rubatto, D., Darling, J., Cenki-Tok, B., Zucali, M., & Engi, M. (2014). Multiple metamorphic stages within an eclogite-facies terrane (Sesia Zone, Western Alps) revealed by Th-U-Pb petrochronology. *Journal of Petrology*, 55(7), 1429–1456. <https://doi.org/10.1093/petrology/egu029>
- Replumaz, A., Negro, A. M., Guillot, S., & Villaseñor, A. (2010). Multiple episodes of continental subduction during India/Asia convergence: Insight from seismic tomography and tectonic reconstruction. *Tectonophysics*, 483(1–2), 125–134. <https://doi.org/10.1016/j.tecto.2009.10.007>
- Reston, T. J., & Manatschal, G. (2011). Rifted margins: Building blocks of later collision. In Brown, D., & Ryan, P. D. (Eds.), *Arc-continent collision* (pp. 3–22). Berlin, Heidelberg: Springer.
- Rubatto, D., Gebauer, D., & Compagnoni, R. (1997). Dating the UHP/HP metamorphism in the Western Alps (Sesia-Lanzo and Zermatt-Saas-Fee): Evidences for subduction events at the Cretaceous-Tertiary boundary and in the Middle Eocene. *Terra Nova Abstract Supplement*, 1, 30.
- Rubatto, D., & Hermann, J. (2007). Zircon behaviour in deeply subducted rocks. *Elements*, 3(1), 31–35. <https://doi.org/10.2113/gselements.3.1.31>
- Rubatto, D., Regis, D., Hermann, J., Boston, K., Engi, M., Beltrando, M., et al. (2011). Yo-Yo subduction recorded by accessory minerals (Sesia Zone, Western Alps). *Nature Geoscience*, 4(5), 338–342. <https://doi.org/10.1038/ngeo1124>
- Schmid, S. M., Kissling, E., Diehl, T., van Hinsbergen, D. J. J., & Molli, G. (2017). Ivrea mantle wedge, arc of the Western Alps, and kinematic evolution of the Alps-Apennines orogenic system. *Swiss Journal of Geosciences*, 110(2), 581–612. <https://doi.org/10.1007/s00015-016-0237-0>
- Seitz, S., Baumgartner, L. P., Bouvier, A.-S., Putlitz, B., & Vennemann, T. (2016). Quartz reference materials for oxygen isotope analysis by SIMS. *Geostandards and Geoanalytical Research*, 41, 69–75. <https://doi.org/10.1111/ggr.12133>
- Soret, M., Agard, P., Dubacq, B., Vitale-Brovarone, A., Monié, P., Chauvet, A., et al. (2016). Strain localization and fluid infiltration in the mantle wedge during subduction initiation: Evidence from the base of the New Caledonia ophiolite. *Lithos*, 244, 1–19. <https://doi.org/10.1016/j.lithos.2015.11.022>
- Vavra, G., Gebauer, D., Schmid, R., & Compston, W. (1996). Multiple zircon growth and recrystallization during polyphase Late Carboniferous to Triassic metamorphism in granulites of the Ivrea Zone (Southern Alps): An ion microprobe (SHRIMP) study. *Contributions to Mineralogy and Petrology*, 122(4), 337–358. <https://doi.org/10.1007/s004100050132>
- Wain, A. L., Waters, D. J., & Austrheim, H. (2001). Metastability of granulites and processes of eclogitisation in the UHP region of western Norway. *Journal of Metamorphic Geology*, 19(5), 609–623. <https://doi.org/10.1046/j.0263-4929.2001.00333.x>
- Walsh, E. O., & Hacker, B. R. (2004). The fate of subducted continental margins: Two-stage exhumation of the high-pressure to ultrahigh-pressure Western Gneiss Region, Norway. *Journal of Metamorphic Geology*, 22(7), 671–687. <https://doi.org/10.1111/j.1525-1314.2004.00541.x>
- Warren, C. J., Beaumont, C., & Jamieson, R. A. (2008). Formation and exhumation of ultra-high-pressure rocks during continental collision: Role of detachment in the subduction channel. *Geochemistry Geophysics Geosystems*, 9, Q04019. <https://doi.org/10.1029/2007GC001839>
- Weber, S., Sandmann, S., Miladinova, I., Fonseca, R. O. C., Froitzheim, N., Münker, C., et al. (2015). Dating the initiation of Piemonte-Liguria Ocean subduction: Lu-Hf garnet chronometry of eclogites from the Theodul Glacier Unit (Zermatt-Saas zone, Switzerland). *Swiss Journal of Geosciences*, 108(2–3), 183–199. <https://doi.org/10.1007/s00015-015-0180-5>
- Zucali, M. (2011). Coronitic microstructures in patchy eclogitised continental crust: The Lago della Vecchia pre-Alpine metagranite (Sesia-Lanzo Zone, Western Italian Alps). *Journal of the Virtual Explorer*, 38, 5. <https://doi.org/10.3809/jvirtex.2011.00286>
- Zucali, M., Spalla, M. I., & Gosso, G. (2002). Strain partitioning and fabric evolution as a correlation tool: The example of the Eclogitic Micaschists Complex in the Sesia-Lanzo Zone (Monte Mucrone-Monte Mars, Western Alps, Italy). *Schweizerische Mineralogische Und Petrographische Mitteilungen*, 82, 429–454.